RESEARCH ARTICLE

Development of Fast Release Aminated Tamarind Gum Carrier-based Solid Dispersion containing Tablets of Ketoconazole for Solubility and Dissolution Rate Enhancement

Atish B Velhal*, Vijay R Salunkhe

KES's, Rajarambapu College of Pharmacy, Sangli, Maharashtra, India.

Received: 20th August, 2022; Revised: 29th September, 2023; Accepted: 07th October, 2023; Available Online: 25th December, 2023

ABSTRACT

This work enhances the solubility as well as dissolution of the biopharmaceutical classification system (BCS) II drug ketoconazole (KTZ) using fast-dissolving tablets that contain solid aminated tamarind gum (ATG). In the first stage amination of the tamarind gum was done to form ATG and which was confirmed by the presence of characteristic peaks using Fourier-transform infrared spectroscopy (FTIR). DSC-TGA analysis showed a weight loss with 3.91% at 100°C, 54.42% loss at 235 to 425°C and 90% at 485°C. The proton nuclear magnetic resonance (^{1}H-NMR) showed all resonance peaks observed in ATG. The XRD analysis of ATG confirmed the amorphous nature of the material. The second phase involved developing KTZ-loaded solid dispersion (SD) using the kneading process. KTZ SD showed drug content of 94.55 to 97.21%. SD of KTZ manufactured with TG showed 2.55 to 23.82-fold solubility enhancement in water while in case of SD with ATG showed 28.51 to 33.19-fold solubility enhancement. KTZ had a 32% dissolution rate in the pure drug sample, but the SD5 formulation showed a complete release of solid dispersion in 120 minutes. In FTIR, the disappearance of the peak signifies the production of solid dispersion and the drug's transformation from a crystalline to an amorphous state. Powder X-ray diffraction (PXRD) analysis of solid dispersions reveals a notable decline in crystallinity, as shown by the removal of strong, distinguishing peaks. The scanning electron microscope (SEM) analysis confirmed the successful development of the SD in which KTZ was observed to be dispersed in a polymeric carrier. Optimized KTZ-loaded SD were utilized in fast-dissolving tablets as the third phase. When compared to the drug release achieved from solid dispersions, it was discovered that the dissolving characteristics of all formulation batches were improved.

Keywords: Ketoconazole, Solubility, Tamarind gum, Aminated tamarind gum.

International Journal of Drug Delivery Technology (2023); DOI: 10.25258/ijddt.13.4.31

How to cite this article: Velhal AB, Salunkhe VR. Development of Fast Release Aminated Tamarind Gum Carrier-based Solid Dispersion containing Tablets of Ketoconazole for Solubility and Dissolution Rate Enhancement. International Journal of Drug Delivery Technology. 2023;13(4):1310-1320.

Source of support: Nil.

Conflict of interest: None

INTRODUCTION

Ketoconazole (KTZ), an imidazole class synthetic antifungal drug with two nitrogen atoms in the five-membered azole ring, has a broad spectrum of activity. It is used in the treatment of superficial as well as systemic fungal infections. KTZ is categorized as a Biopharmaceutical classification system (BCS) II drug due to higher permeation and characteristics of dissolution and absorption but its application is restricted due to the solubility issues. KTZ has a low bioavailability due to its restricted solubility in water, which eventually reduces how effective it is at treating infections.[1,2]

It is essential to design appropriate pharmacological formulations in order to address this serious problem. Poorly soluble medications, such as ketoconazole can be dissolved or dispersed in formulations known as solid dispersions. This approach improves drug solubility and dissolution rate, ultimately enhancing bioavailability.[3] In order to do this, solid dispersions change the drug's crystalline structure, increase the amount of surface area accessible for dissolution, enhance wetting and spreading in the dissolution media, create drug-polymer complexes, and increase drug mobility. These methods enable the medicine to dissolve more quickly and have better solubility.[4] Overall, solid dispersions provide a useful method for overcoming the problems posed by BCS II drugs, improving their therapeutic effectiveness.

In comparison to manufactured polymers, natural polymers that come from plants and animals have advantages. They have a lower environmental impact because they are sustainable, renewable, and biodegradable.[5,6] Tamarind gum polysaccharide (TGP) is one of the natural polymers that has great biocompatibility and low toxicity, making it useful for biomedical applications.

Author for Correspondence: atishvelhal@gmail.com

TGP is a naturally occurring polysaccharide obtained from the seed endosperms of the Fabaceae plant *Tamarindus indica* Linn. It is water soluble having a large molecular weight of 1735 kDa. TGP is a branched, nonionic polysaccharide that forms gels and adheres to mucous membranes. It is non-irritating, non-carcinogenic, biodegradable, and biocompatible.[7,8] TGP is a potential biopolymer that has uses in the food, cosmetics, and pharmaceutical industries. Numerous medication delivery methods, including oral, intestinal, ocular, buccal, and nasal routes, have used it as an excipient after significant investigation.[9]

Despite being frequently employed in drug delivery formulations, tamarind gum (TG) suffers from few limitations like an unpleasant smell, poor water solubility, and a quick rate of degradation in aquatic settings. To get over these restrictions, TG has undergone several chemical treatments using functional groups such as carboxymethyl, amine, and thiol.[10] Modified tamarind gums like aminated tamarind gum (ATG) provide increased mechanical characteristics, decreased degradability, and improved stability. The aminated tamarind gum has many benefits over the tamarind gum. It offers various benefits in terms of water solubility, rheological properties, stability, and functionality. Controlled drug release, greater adhesion, increased bioavailability, targeted administration, and surface modification for drug loading are all possible with its flexible approach to drug delivery systems.[11-13] These formulations may enhance patient outcomes, optimize medication delivery profiles, and improve treatment efficacy. However, there hasn't been much research done on the use of ATG in solid dispersion. We believe, based on a thorough review of the literature, that ATG can be utilized in solid dispersions to improve the solubility, stability, controlled drug release, and bioavailability of poorly soluble medicines. It allows for controlled release by adjusting concentration or crosslinking. ATG is compatible with common excipients and can be easily processed.[14-18]

Overall, the use of ATG in solid dispersions provides a flexible solution to problems with solubility and enhances drug delivery. We have performed this effort to use the ATG in the solid dispersion with higher solubilities and dissolutions through fast-dissolving tablets in light of all these potential benefits of the ATG.

MATERIALS AND METHODS

Materials

Ketoconazole was gifted by SD Chemicals, Mumbai tamarind kernel powder/gum (TG) was obtained as a gift from Chhaya Industries, Barshi, Maharashtra. Ethylene diamine, sodium hydroxide, ethanol, and sodium borohydride was purchased from Loba Chemicals, Mumbai. Neusilin was gifted by Gangwal Chemicals, Mumbai

Synthesis of ATG

In an aqueous medium at 3°C for 6 hours, a 100 mL solution of TSP (2%, w/v) was combined with 0.8 mL of ethylene diamine (40%, w/w of polymer). After that, over a period of two hours, sodium borohydride ($NaBH_4$) was gradually added until a thick gel had formed. After the material precipitated, 300 mL of ethyl alcohol (95%, v/v) was used to wash it multiple times. The precipitates were filtered, dried for three hours at 70°C and ground into homogeneous particles.

Characterization of ATG

Organoleptic characteristics of ATG particles

Color, odor, taste and shape of the particles was observed by microscope.

Identification test

- *Solubility determination*

Solubility was checked in ethanol, methanol, acetone, and benzene

- *pH determination*

By using pH meter, pH of the sample was determined

ATR-FTIR of ATG

IR spectra of ATG was recorded using ATR-FTIR The ATG sample was kept onto the ATR and the spectrum was recorded from 600 to 3500 cm^{-1}.

DSC-TGA of ATG

TGA and DSC of ATG was performed using the thermogravimetric analyzer. The sample was heated from 30 to 500°C at the rate of 10°C/min, under a nitrogen atmosphere

^{1}H-NMR of ATG

^{1}H-NMR of ATG was measured using an NMR spectrophotometer operating at 400 MHz (contact time of 3.5 ms, a relaxation delay of 5s, sweep width of 35 kHz and spinning speed of 10 KHz).

X-ray powder diffraction

X-ray powder diffraction (XRD) pattern of ATG was recorded using an X-ray diffractometer with a copper target, operated at a voltage of 30 kV, 30 mA current, at 2°C/min scanning speed.

Preparation of SD using the Kneading Method

Comparative preparation of SD of KTZ in ATG and tamarind gum was made by kneading method with ratios of 1:1, 1:2, and 1:3 ratio (Table 1). The appropriate quantity of methanol allowed the necessary amount of KTZ to dissolve. The needed amount of ATG was then added to this, and the drug solution was stirred continuously in the mortar for 30 minutes. The solvent then vanished, leaving the material to solidify. The substance was crushed up, dried, and passed through filter number 80. After being characterized, the obtained solid dispersions kept in airtight containers.

Table 1: Composition of various batches of solid dispersion containing ATG and tamarind gum mixture

Batch code	*Composition*	*Ratio*
S. D1	Ketoconazole: Tamarind gum	1:1
S. D2	Ketoconazole: Tamarind gum	1:2
S. D3	Ketoconazole: Tamarind gum	1:3
S. D4	Ketoconazole: Aminated tamarind gum	1:1
S. D5	Ketoconazole: Aminated tamarind gum	1:2
S. D6	Ketoconazole: Aminated tamarind gum	1:3

Characterization of Ketoconazole Aminated Tamarind Gum Solid Dispersion

Drug content

A solid dispersion containing 10 mg of the KTZ was dissolved in a flask, and 25 mL of methanol was added. The solution was agitated in a centrifuge for 60 minutes. The mixture was filtered, and appropriately diluted with methanol, and the presence of drugs was assessed using a UV spectrophotometer. Using methanol as a blank, the drug content was calculated using UV spectrophotometry.

Percentage yield

The formula below was used to compute the percentage yield from F1 to F6.

%Yield = Wt of SD/ Wt of drug and polymer X 100

Saturation solubility

Extra plain KTZ was added to separate glass-stoppered flasks with 10 cc of distilled water. A magnetic stirrer was used to agitate the samples at 37°C and 100 rpm for 24 hours, or until equilibrium was reached. Filtrates were properly diluted with distilled water before being measured spectrophotometrically at 238 nm.

Fourier transform infrared studies

Fourier transform infrared (FTIR) spectrophotometer. Was used for the analysis. A little sample was obtained and placed right on the IR platform. Then, spectra for solid dispersion complexes, tamarind gum, tamarind gum that had been amined, and pure KTZ were captured. A 400 to 4000 cm scanning range was used.

Dynamic scanning calorimetry

Dynamic scanning calorimetry (DSC) analysis was done using a DSC calorimetry device, and thermograms of pure KTZ, tamarind gum, tamarind gum that has been amined, and solid dispersion formulation SD 5 were recorded. The samples were kept in an aluminum pan and heated (25–500°C) while being exposed to a nitrogen environment flowing at a rate of 10mL/min.

Powder X-ray diffraction

Powder X-ray diffraction (P-XRD) was performed to look for any crystallinity. The powdered test sample was placed in an aluminum test container with a 2.5 cm square and a 0.5 mm depth.

Dissolution study

The powdered test sample was placed in an aluminum test container with a 2.5 cm square and a 0.5 mm depth. At 37 ± 0.5°C and 50 rpm, SD corresponding to 20 mg of KTZ were added to 900 mL of phosphate buffer (pH 6.8). At predetermined intervals, 5 mL aliquots were taken out and filtered to get clear solution. To preserve the dissolution medium volume, an equivalent volume of brand-new dissolution medium was substituted. At 261 nm, the filtered samples underwent spectrophotometric analysis.

Antifungal study

Cup plate method was employed to assess the antifungal efficacy of the optimized SD, pure KTZ, and ATG against *Candida albicans*. *C. albicans* inoculum was evenly distributed on Sabouraud's dextrose agar, allowing it to solidify in the petri dish. Following agar solidification, sterile borers (5 mm) were used to create cups. Subsequently, 0.5 mL of the SD solution was added to one cup, while 0.5 mL of pure KTZ and ATG were added to separate cups. The plate was then placed in an incubator at 37°C for 24 hours. The zone of inhibition was measured and compared across the different samples.

Formulation of Ketoconazole Tablet

Tablets equivalent to 50 mg of KTZ were prepared using Neusilin and microcrystalline cellulose through DC technique. Materials were sieved using #40 sieve and dried at a temperature of 40 to 45ºC to remove moisture. The weighed amounts of the drug and other ingredients, except for magnesium stearate and talc, were manually mixed using the geometric addition method for a duration of 20 minutes. The magnesium stearate and talc passed through a #60 sieve, and mixed, in addition to blending thoroughly with the preliminary combination. The blend was then compressed with KBR Press. Table 2 lists the components of several tablet formulations.

Evaluation of Powder Mixed Blend of Drug and Excipient

Bulk density

By gently pouring a known amount of powder sample through a glass funnel and into a graduated measuring cylinder, bulk density (BD) was determined using the following formula.

$$BD = \frac{\text{mass of material (gm)}}{\text{volume (mL)}}$$

Tapped density

Tapped density (TD) of the powder mixture was determined by gently poured a known quantity of the powder sample into a glass funnel, which was placed on top of a graduated measuring cylinder. The measuring cylinder was then imperiled towards 100 taps to settle the powder. The volumes engaged *via* the settled powder samples were recorded. The TD was calculated utilizing the following equation.

$$TD = \frac{\text{Weight of sample in gm}}{\text{tapped volume (mL)}}$$

Compressibility index

The following equation was used to calculate Compressibility index (CI)

$$CI = \frac{TD - BD}{TD} X\ 100$$

Angle of repose

It was determined using the funnel technique. Lubricated granules was placed in a funnel and attuned towards a specific height so that the powder shaped a heap that reached the funnel's tip. The angle of repose was determined utilizing the below formula.

$$\tan\theta = \frac{h}{r}$$

Hausner's ratio

Hausner's ratio (HR) is a significant parameter used towards assessing the flow characteristics of powders and granules. It is determined utilizing the subsequent formula.

$$HR = \frac{TD}{BD}$$

Evaluation of Tablets

Tablet thickness

The purpose of this test was to calculate the variation in tablet thickness which was measured by using a screw gauge.

Weight variation

As per the Indian Pharmacopoeia (IP) guidelines, the test was performed on 20 tablets. The average weight was calculated by weighing the individual tablets on a digital balance. Weight variation was determined considering the individual tablet weight and average weight.

Hardness

This test provides an indication of the tablets' mechanical strength and resistance to breakage. A Monsanto hardness tester was used to determine the hardness.

Friability

Friability testing was conducted using Roche's friability. Tablets were kept to abrasion and in a plastic chamber that revolves at 25 rpm. During each revolution, the tablets are dropped from a height of 6 inches. After the test, the tablets were de-dusted and reweighed to determine the percentage of weight loss due to friability.

% Friability = Initial wt – Final wt/ Initial wt X 100

Content uniformity

The drug content of fast-dissolving tablets containing KTZ was assessed by weighing and finely powdering 10 tablets from each formulation. The samples were analyzed at 238 nm and KTZ content was determined. This involved diluting a sample of the powder, equivalent to 20 mg of KTZ, in methanol to create a solution for analysis.

In-vitro disintegration time

The most common cause of FDT disintegration was water uptake by the disintegrant by capillary action, which causes swelling and tablet disintegration. Additionally, it was discovered that a higher compaction force could alter the disintegration time. Using the electro lab disintegration equipment USP, a disintegration investigation on six tablets was conducted for the current study. The tablets were placed in the apparatus, and distilled water at 37 ± 2°C was utilized as the disintegrating medium. The amount of time required for the tablets to completely dissolve, leaving no palpable mass inside the device, was recorded in seconds.

Dissolution study

The USP type-II dissolution apparatus consisting of 900 mL of phosphate buffer pH 6.8 at 37 ± 0.5°C and a paddle stirrer running at 50 rpm was used. Each test involved one pill. Ten mL portions of the dissolving liquid were taken out at predetermined intervals between five and sixty minutes. A similar volume of brand-new media was used in place of the removed samples. The specimens were subsequently passed through a 0.45 m membrane filter paper, and the absorbance at 256 nm was measured in order to analyze them. The cumulative amount of drug dissolved was determined.

Stability studies

The optimized formulation, meeting acceptable criteria for DT, hardness, thickness, weight variation, dissolution, and content uniformity, underwent an accelerated stability study. This involved subjecting the selected formulation to conditions of 40ºC/75% RH for a duration of 3 months.

RESULTS AND DISCUSSION

Organoleptic Characteristics of ATG Particles

ATG powder was light cream brown in color, odorless and tasteless with irregular in shape. ATG was found to be rough in touch, texture, and fracture. Microscopic image of the ATG particles are shown in Figure 1.

Test for carbohydrates was found to be positive and all other remaining tests were negative. It indicates that synthesized ATG was free from any other impurities. The cold water solubility of ATG sample was found to be 10.53 ± 1.28 mg/mL. It indicates amination of tamarind increases the solubility of TG. The sample of ATG was found to be insoluble in ethanol, methanol, acetone, and benzene. pH of 1% ATG sample was found to be 5.94.

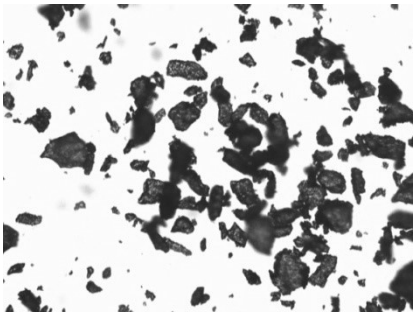

Figure 1: Microscopic image of ATG particles

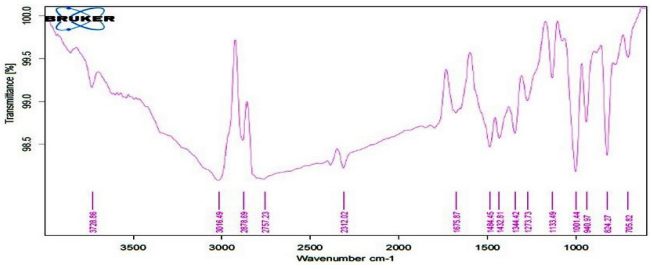

Figure 2: The ATR-FTIR spectrum of ATG

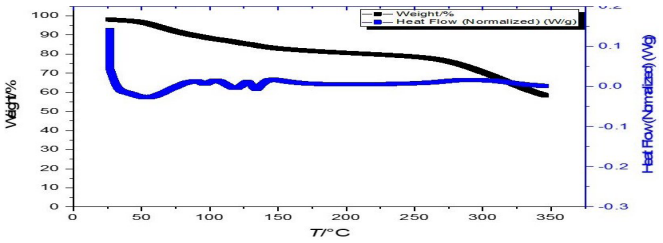

Figure 3: TGA and DSC of ATG

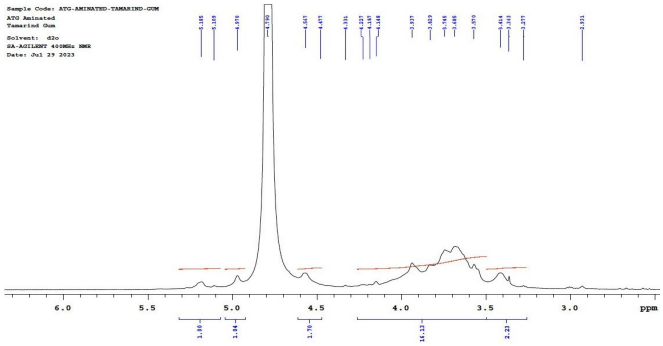

Figure 4: Solid state ^{1}H-NMR of ATG

ATR-FTIR of ATG

In the original tamarind gum, broad bands in the region of 3200 to 3600 cm^{-1}, represent the stretching vibrations of hydroxyl groups (-OH). After amination, the intensity of these bands decreased due to the reaction of amino groups with hydroxyl groups (Figure 2). The appearance of new peaks or bands in the region of 3300 to 3500 cm^{-1} indicated the presence of amino groups (-NH2). These peaks represent N-H stretching vibrations. In the original tamarind gum, band around 1700 to 1750 cm^{-1} represents carbonyl groups (C=O). After amination, changes in the intensity and position of this band are observed in ATG. Bands in the region of 2800 to 3000 cm^{-1} are present due to C-H stretching vibrations. These bands can provide information about the presence of aliphatic and aromatic groups in the molecule. Tamarind gum typically contains ether linkages (C-O-C), in the region of 1000 to 1300 cm^{-1}. Changes in these bands have occurred and indicated modifications in the gum structure. Other functional groups, such as C-N stretching vibrations, which would appear in the region of 1000 to 1500 cm^{-1}. Different IR peaks of the ATG are presented in Figure 2.

DSC-TGA of ATG

Figure 3 presents the DSC-TGA analysis of ATG, revealing its thermal decomposition behavior. The thermal decomposition of ATG starts at 25°C with the initiation of weight loss as shown in the thermograph. Nearly 60% weight loss of ATG has been observed within a temperature range of 25 to 350°C. The initial slow and gradual weight loss was observed due to the escape of bound and free molecules of water associated with polymers. Rapid and significant weight loss was observed from 275 to 350°C. The DSC curve aligns with the weight loss observations from the ATG curve, providing supporting evidence for the thermal decomposition of ATG.

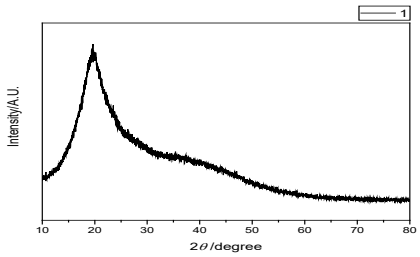

Figure 5: X-ray powder diffraction

^{1}H-NMR of ATG

Signals in the region of 0.5 to 2.5 ppm are typically associated with aliphatic hydrogens (CH and CH2 groups) (Figure 4). These resonances may arise from the hydrocarbon chains in the polymer, as well as any aliphatic groups introduced during the amination process. Hydroxyl groups (-OH) can exhibit broad and often overlapping signals in the region of 2 to 5 ppm. The exact chemical shifts and shapes of these signals may vary depending on number and environment of the hydroxyl group within ATG. The introduction of amino groups (NH_2) during amination may result in signals in the region of 0.5 to 3 ppm, depending on the specific chemical structure of the amino groups and their proximity to other functional groups. These signals can be broad and may overlap with other resonances. Carbonyl groups (C=O) may appear as signals in the region of 1 to 3 ppm, depending on their specific chemical environment within the polymer structure. Carbon atoms associated with ether linkages (C-O-C) may exhibit signals in the region of 3 to 4 ppm. Hydrogens attached to quaternary carbon atoms (CH_3 groups) might appear in the region of 0.5 to 2 ppm, depending on their local environment within the polymer structure (Figure 4).

P-XRD

The XRD pattern of ATG typically exhibits a diffuse scattering pattern without distinct, sharp peaks (Figure 5). This pattern strongly indicates that ATG primarily possesses an amorphous nature, lacking well-defined crystalline regions. The absence of discernible peaks is indicative of a random arrangement of polymer chains, resulting in a disordered molecular structure. The broad, diffuse halo peak observed in the XRD pattern serves as a clear indicator of ATG's amorphous character. The position and width of this peak can provide valuable insights into the average molecular spacing and the degree of disorder within the polymer chains. The presence or absence of a weak, broad peak in the XRD pattern can convey information about the degree of crystallinity present in ATG. If a weak peak is observed, it suggests the presence of small crystalline regions within the amorphous matrix, indicating a relatively low degree of crystallinity. Conversely, a completely amorphous XRD pattern, devoid of any discernible peaks, signifies a higher degree of amorphousness and the absence of crystalline regions.

Development of KTZ-loaded SD

ATG was used as a carrier for solid dispersions using the kneading method. The kneading method involves mechanically

Table 3: Comparative yield of the SD formulated using kneading method

Batch code	*Composition*	*Ratio*	*%Yield*	*%Drug content*
SD1	KTZ: TG	1:1	94.10	94.55
SD2	KTZ: TG	1:2	94.39	94.71
SD3	KTZ: TG	1:3	96.25	95.20
SD4	KTZ: ATG	1:1	97.81	97.21
SD5	KTZ: ATG	1:2	97.11	96.65
SD6	KTZ: ATG	1:3	95.62	97.01

Table 4: Saturation solubility data of the KTZ and SD formulations in distilled water

Batch code	*Formulation/ components*	*Ratio*	*Solubility (mg/mL)*	*Fold enhancement*
---	Pure KTZ	---	0.047	……
SD1	KTZ: TG	1:1	0.12	2.55
SD2	KTZ: TG	1:2	0.85	18.08
SD3	KTZ: TG	1:3	1.12	23.82
SD4	KTZ: ATG	1:1	1.34	28.51
SD5	KTZ: ATG	1:2	1.56	33.19
SD6	KTZ: ATG	1:3	1.43	30.42

combining the medication and carrier while being in the presence of an appropriate solvent. ATG, a hydrophilic polymer, has the capacity to improve the solubility of drugs that aren't very water-soluble. The drug particles are effectively disseminated and stabilized throughout the kneading process by dispersing them inside the ATG matrix, leading to increased dissolution rates and bioavailability

%Yield and drug content of SD

All formulation batches using TG and ATG showed a greater SD yield. The yield's specifics are shown in Table 3. The range of the SD's yield was between 94.1 and 97.81%. The greater yield showed that there was little to no excipient and medication loss during the production process. The lengthy and vigorous mechanical mixing of the medication and polymer occurs during the kneading step.[19] Stronger drug-polymer interactions are made possible by the enhanced contact between the drug and polymer caused by this mechanical force. This enhanced contact encourages drug dispersion within the matrix of the polymer and improves medication solubility. The better yield shown in solid dispersions made using this process is mostly due to the improved drug-polymer interaction, smaller particle size, homogenous distribution, and higher drug solubility.

Furthermore, all of the batches that were developed had a greater drug concentration for the SD (94.55–97.21%). The medication is distributed more uniformly throughout the polymer matrix thanks to the kneading process. This uniform distribution of the medication throughout all units of the solid dispersion guarantees that each unit contains roughly the same amount of the drug, resulting in predictable drug release patterns and enhanced content uniformity.

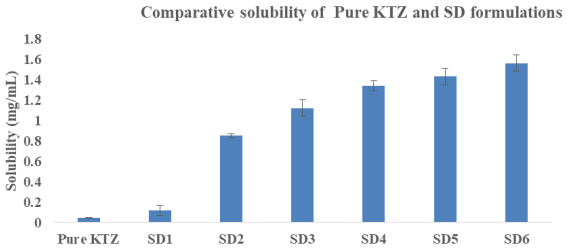

Figure 6: Comparative saturation solubility of KTZ and SD in distleed water

Saturation solubility determination

With distilled water, the saturation solubility of pure KTZ and KTZ loaded with SD was evaluated. When compared to pure KTZ, SD formulations significantly improved solubility. In Table 4 and Figure 6, the data on comparative solubility are displayed.

SD of KTZ manufactured with TG showed 2.55 to 23.82-fold solubility enhancement in water while in case of SD with ATG showed 28.51 to 33.19-fold solubility enhancement. It has been determined with certainty that the ATG, as opposed to TG, has a better ability to increase the solubility of the KTZ. Because their chemical structures or functional groups differ, ATG may have stronger interactions with KTZ than TG. This improved contact may encourage improved medication dispersion and raise the drug's solubility in the solid dispersion. Additionally, ATG may have better wetting and dispersion qualities than TG. This may improve KTZ's Dispersibility in the solid dispersion, increasing the amount of drug surface area that is available for dissolving and improving solubility. Additionally, ATG might possess extra chemical or functional groups that promote the solubilization of drugs. These characteristics may facilitate interactions with KTZ and enhance their solubility in solid dispersion.

In-vitro dissolution studies

The comparative dissolution profile of KTZ and SD formulations is shown in Figure 7. KTZ had a 32% dissolution rate in the pure drug sample, but the SD5 formulation showed complete release of solid dispersion in 120 minutes.

The SDs formulated with ATG showed rapid release profile in comparison to the SDs of TG

The 1:1 ratio of the SD4 formulation was discovered to be optimal for formulating the SD of KTZ. In comparison to TG, ATG in solid dispersions with KTZ demonstrates better wetting, dispersibility, and drug-polymer interaction.[20] By boosting drug solubilization, expanding surface area, and enhancing drug dispersion, it improves medication release. The supersaturated condition of KTZ is stabilized by ATG, increasing the effective drug concentration and accelerating drug dissolution. Better miscibility ensures uniform drug distribution, facilitating improved solubility and dissolution rates. With the help of its functional groups, which encourage drug solubilization and dispersion in the dissolving media, ATG's special features aid in rapid dissolution. Overall, KTZ dissolution kinetics are improved by ATG solid dispersions.

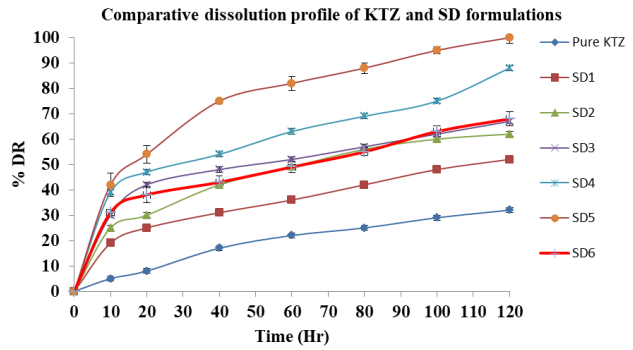

Figure 7: Comparative dissolution profile of KTZ and SD formulations

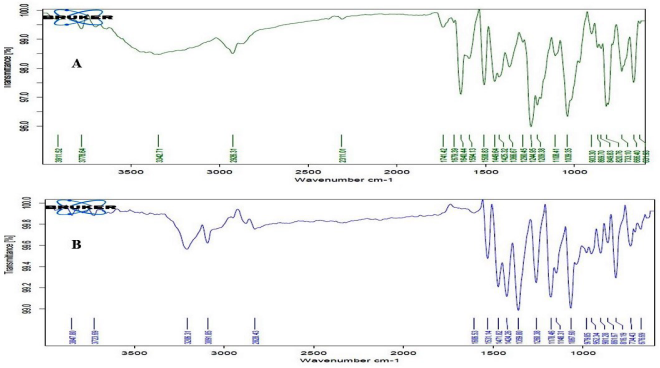

Figure 8: FTIR spectra of A: Pure KTZ and B: SD of KTZ

At higher concentrations, ATG in solid dispersions of KTZ forms a dense polymer matrix that hinders drug release by creating a diffusion barrier. Drug diffusion is further impeded by the dissolution medium's increased viscosity, which slows dissolution. Stronger polymer-drug interactions impede drug release by limiting dissolution and diffusion. At higher concentrations ATG slower the dissolution

FTIR analysis of KTZ SD

The FTIR spectrum of pure VRZ typically showed a sharp peak in the range of 1680 to 1750 cm^{-1} indicating the presence of carbonyl group (C=O) found in KTZ, which is part of the imidazole ring (Figure 8A). Peaks in the range of 1600 to 1500 cm^{-1}, represent aromatic C=C bonds present in the imidazole and other aromatic rings in the molecule. In the fingerprint region (below 1500 cm^{-1}) the characteristic peaks belong to various functional groups or vibrations involving aliphatic (alkyl) groups in the molecule. Peaks due to N-H stretching vibrations are present in the range of 3200 to 3500 cm^{-1}. KTZ also has other functional groups, such as oxygen-containing groups like ethers or alcohols and these peaks are present in the 1000 to 1300 cm^{-1} for C-O bonds. Similar peaks were also observed in FTIR spectra of solid dispersion (Figure 8B).

DSC analysis of KTZ SD

DSC is a valuable tool in drug development, enabling the identification of critical transitions such as melting, glass transition, and crystallization. In Figures 9A and 9B, DSC thermograms are presented for pure KTZ and the SD5

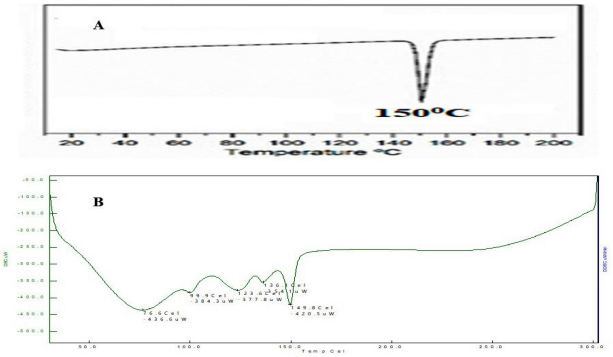

Figure 9: DSC thermogram of A: Pure KTZ and B: Solid dispersion SD5

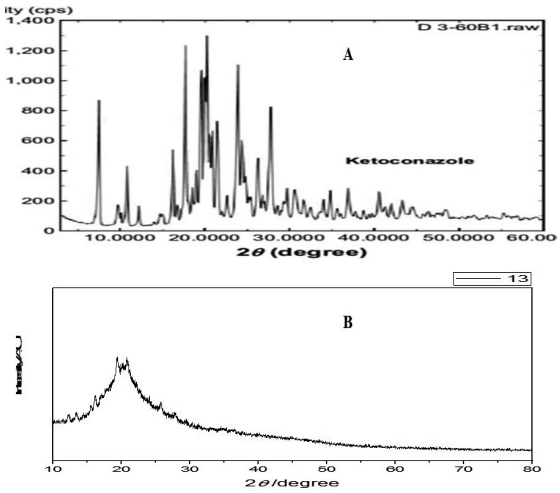

Figure 10: X ray diffraction pattern of (A): Pure KTZ drug and (B): SD5 formulation

formulation, respectively. In the DSC analysis of pure KTZ, a distinct and sharp endothermic peak is observed at approximately 150°C. This peak indicates the highly crystalline nature of pure KTZ. For pure KTZ, its DSC thermogram reveals a melting point within the range of 148 to 152°C, consistent with its known characteristics. However, when examining the DSC thermogram of the SD5 formulation, an endothermic peak is detected at approximately 149.8°C. Notably, the intensity of the endothermic peak corresponding to KTZ is reduced in the SD5 formulation. This reduction in peak intensity suggests an increase in the amorphous nature of KTZ within the SD formulation.

X-ray diffraction

The XRD spectrum presented in Figure 10(A) shows distinct and sharp peaks of KTZ at diffraction angles of 10.00, 15.75, 20.00, 25.50, 28.30, 30.64, 35.40, 39.57, 40.00, 45.90, 50.11 degrees. This indicates the crystalline nature of pure KTZ. However, in the SD5 formulation shown in Figure 10(B), the intensity of the crystalline peaks of KTZ is significantly reduced. This indicates that KTZ in the final formulation exists in an amorphous form. These observations provide clear evidence that the solid dispersion formulation successfully transformed KTZ from its crystalline state to an amorphous state.

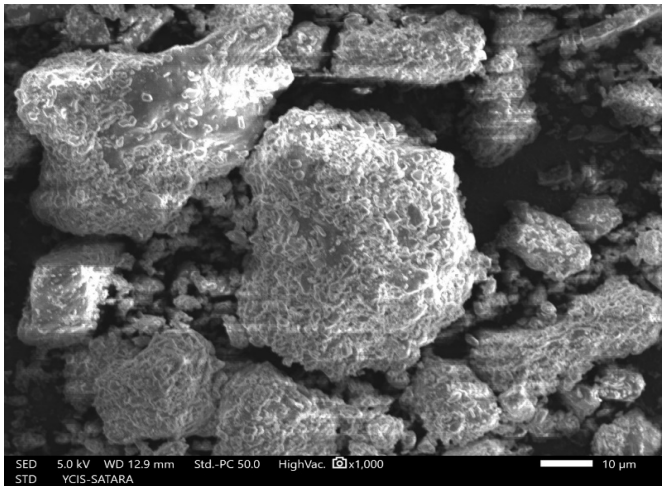

Figure 11: SEM of KTZ-loaded ATG solid dispersion

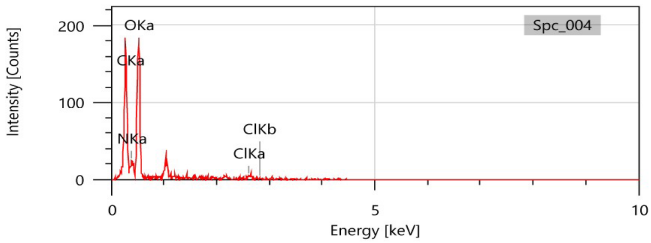

Figure 12: EDS analysis of SD5 formulation with intensity count and energy

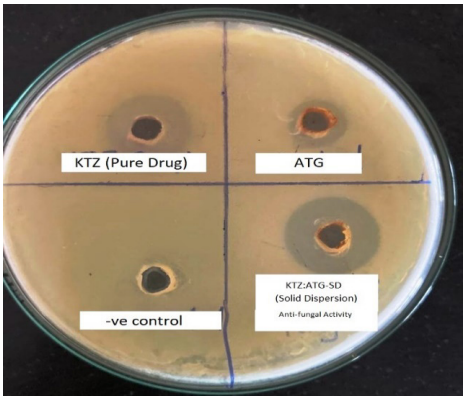

Figure 13: comparative antifungal activity of pure KTZ, ATG and KTZ-loaded ATG solid dispersion

SEM analysis of KTZ SD

The SEM image revealed that the KTZ-loaded ATG solid dispersion exhibited a distinct morphology compared to the pure components. The dispersed particles of KTZ appeared as small, irregularly shaped particles embedded within the ATG matrix (Figure 11). The ATG matrix appeared as a continuous, amorphous structure surrounding the drug particles. The SEM analysis confirmed the successful formation of the solid dispersion, where the drug was dispersed within the polymeric carrier. Overall, the SEM analysis demonstrated the effectiveness of the ATG carrier in dispersing KTZ and forming a solid dispersion.

Table 5: Flow properties of the lubricated blend containing SD of VRZ

Batch	*BD (gm/mL)*	*TD (gm/mL)*	*CI (%)*	*HR*	*Angle of repose*
F1	0.41 ± 0.001	0.66 ± 0.002	23.61 ± 0.11	1.06 ± 0.003	24.17 ± 0.14
F2	0.44 ± 0.004	0.61 ± 0.001	24.57 ± 0.2	1.12+0.002	34.61 ± 0.22
F3	0.43 ± 0.04	0.64 ± 0.003	16.57+0.8	1.11+0.003	39.32 ± 0.32
F4	0.45 ± 0.003	0.66 ± 0.006	16.49+0.11	1.14+0.002	37.62 ± 0.12
F5	0.60 ± 0.03	0.83 ± 0.002	18.62 ± 0.1	1.13 ± 0.003	26.01 ± 0.24
F6	0.77 ± 0.02	0.82 ± 0.002	20.62+0.12	1.15+0.003	28.41+0.11
F7	0.37 ± 0.01	0.68+0.001	18.13 ± 0.22	1.12 ± 0.004	31.13 ± 0.26
F8	0.45 ± 0.02	0.64 ± 0.003	22.27 ± 0.15	1.20 ± 0.003	27.27 ± 0.32

Table 6: Comparative physicochemical properties of the compressed tablets

Batch	*Thickness (mm)*	*Diameter (mm)*	*Hardness (kg/cm^2)*	*Friability (%)*	*Weight variation*	*Content uniformity*	*DT*
F1	1.98 ± 0.087	10.01 ± 0.02	4.76 ± 0.85	0.15	300.80 ± 0.26	95.94 ± 1.10	90.32 ± 1.62
F2	2.10 ± 0.4	10.01 ± 0.01	4.95 ± 0.05	0.22	302.02 ± 1.65	96.92 ± 1.42	78.15 ± 1.0
F3	1.69 ± 0.15	10.02 ± 0.01	4.20 ± 0.25	0.17	300.92 ± 1.05	94.86 ± 1.72	79.01 ± 1.2
F4	2.12 ± 0.17	10.03 ± 0.02	4.25 ± 0.15	0.29	301.60 ± 0.09	96.11 ± 1.30	67.35 ± 2.0
F5	2.17 ± 0.08	10.05 ± 0.01	5.47 ± 0.10	0.23	300.50 ± 0.85	100.25 ± 0.89	58.47 ± 1.0
F6	2.19 ± 0.15	10.04 ± 0.01	5.10 ± 0.01	0.15	300.25 ± 0.07	96.67 ± 1.26	68.32 ± 1.4
F7	2.08 ± 0.06	10.0 ± 0.05	4.25 ± 0.18	0.26	301.10 ± 0.02	99.68 ± 1.12	75.25 ± 2.0
F8	3.01 ± 0.057	10.05 ± 0.04	4.90 ± 0.76	0.30	301.24 ± 0.99	99.78 ± 1.27	80.11 ± 1.5

Table 7: Comparative dissolution profile of fast-dissolving tablets containing KTZ SD

Time (min)	*Formulation*							
	F1	*F2*	*F3*	*F4*	*F5*	*F6*	*F7*	*F8*
0	0	0	0	0	0	0	0	0
5	15	19	25	34	39	36	26	22
10	20	24	33	39	47	41	35	29
15	24	35	39	47	55	48	42	37
20	35	42	47	56	65	60	48	44
30	42	48	55	62	82	65	55	50
40	50	57	65	72	89	70	59	54
60	54	64	78	85	100	75	64	59

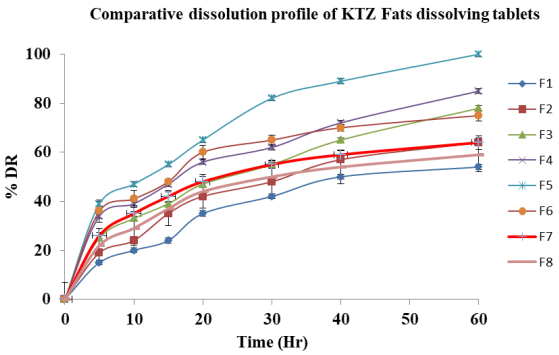

Figure 14: Comparative dissolution profile of KTZ from fast dissolving tablets

Table 8: Stability studies of F5 formulation stored at 40ºC/75% RH

Sr. no.	*Parameters (F5)*	*40ºC/75%RH*			
		Initial	*1M*	*2M*	*3M*
1	Disintegration time in water (sec)	58.47 ± 1.0	55.50 ± 1.2	57.45 ± 1.1	58.10 ± 1.1
2	Hardness (kg/cm2)	5.47 ± 0.10	5.5 ± 0.17	6.5 ± 0.11	6.0 ± 0.14
3	Thickness (mm)	2.17 ± 0.08	3.17 ± 0.09	4.20 ± 0.09	4.20 ± 0.11
4	Weight variation (%)	300.50 ± 0.85	299.5 ± 0.17	301.18 ± 0.27	302.24 ± 0.78
5	Content uniformity (%)	100.25 ± 0.89	99.8 ± 0.45	99.5 ± 0.41	99.8 ± 0.72
6	DR at 60 min (%)	100	99.0	98.5	99.0

Energy-dispersive X-ray analysis

Energy-dispersive X-ray analysis (EDX) or EDS is a technique used to determine the elemental composition of a sample. In the case KTZ loaded into ATG solid dispersion, EDX analysis provided insights into the distribution and concentration of elements present. The specific elements present in the solid dispersion using EDS are carbon (C), oxygen (O), nitrogen (N), and hydrogen (H), which are basic elements of any molecule. The presence of any additional elements that are not part of the aminated tamarind gum's natural composition, is chlorine (Cl) is also detected due to presence of KTZ. These observations confirmed that KTZ has been successfully loaded into the solid dispersion. Various elements with intensity count and energy are presented in Figure 12.

Antifungal activity

The comparative antifungal activity of pure KTZ, ATG and KTZ-loaded ATG solid dispersion is presented in Figure 13. The highest zone of inhibition against *C. albicans* was found to be 27 mm followed by 21 mm in the case of pure KTZ. The ATG also showed a zone of inhibition of 15 mm. These observations clearly indicated that pure KTZ when formulated as a solid dispersion using ATG as a carrier, antifungal activity gets enhanced.[21] ATG has also shown the antifungal activity that might have enhanced the KTZ activity.

Characterization of a Lubricated Blend Containing SD of KTZ

The flow properties of the lubricated blend is represented in Table 5. The angle of repose of the granules was observed between 24.17 ± 0.14 to 39.32 ± 0.32, BD was ranged from 0.37 ± 0.01 to 0. 0.77 ± 0.02 gm/cm^3, TD was found between 0.61 ± 0.001 to 0.83 ± 0.002. HR was ranged from 1.06 ± 0.003 to 1.20 ± 0.003 and CI was found between 16.57+0.8 to 24.57 ± 0.2. When the angle of repose is between 25 and 30, the granules' flow quality is regarded as good enough. High bulk density values were observed in a lubricated blend of batch F5 which is an indication for good flow properties and is directly influenced by the Hausner;s ratio and Car's index. These granules exhibited excellent flow properties that met the compression requirements.

Characterization of Compressed Tablets containing SD of KTZ

Table 6 presents the physicochemical characteristics of the tablets in comparison. The tablets were compressed using a round punch with a 10 mm diameter. Given the proportions of the punch, the tablet's diameter was deemed to be appropriate. Due to the granules' outstanding flow qualities, which result in complete die filling, there was very little weight variation between 300.25 ± 0.07 and 302.02 ± 1.65 and mg. A range of 100.25 ± 0.89 to 94.86 ± 1.72 showed great content uniformity. The tablets' hardness ranged from 4.20 ± 0.25 to 5.25 ± 0.15 kg/cm^2. Tablets were assessed using the Roche friability, and acceptable levels of friability (less than 1%) were found. The tablets' thickness was determined to be between 1.69 ± 0.15 and 3.01 ± 0.057 millimeters (mm) thick. All formulations' in vitro disintegration times were discovered to be in the range of 58.47 ± 1.0 to 90.32 ± 1.62 seconds.

In-vitro dissolution studies of KTZ compressed tablets

Fast-dissolving KTZ tablets were the subject of an *in-vitro* dissolution research in phosphate buffer PH-6.8. In Table 7 and Figure 14, the comparable dissolution profile is displayed.

The dissolution rate was for formulation F5 was found to 100% within 60 minutes. Dissolution was improved due to use of croscarmellose sodium (CCS). F5 was the formulation that had the best fast-dissolving potential, releasing the entire dose in just 60 minutes.

In this study, ATG was synthesized from TG and used as a carrier in the solid dispersion of KTZ. Compared to solid dispersions made just with TG, the solid dispersion made with ATG had better-dissolving characteristics. In comparison to pure KTZ, the modified SD showed improved pharmacokinetic characteristics. This enhancement was attributed to several factors. First off, the amorphous state of KTZ that was attained through dispersion in the ATG polymer matrix boosted the drug's solubility, resulting in faster rates of dissolution. Second, the increased surface area created by the finely dispersed KTZ particles inside the ATG matrix allowed for more effective drug dissolution when the drug came into contact with the dissolving medium.

Stability study

The accelerated stability study for 3 months was conducted on the optimized tablet formulation (F5) at 40ºC/75% RH. Throughout each assessment point, all physicochemical parameters tested demonstrated no notable changes when compared to the initial parameters. The formulation proved to be robust and remained stable over the entire 3-month period. Comparative results of the stability study are detailed in Table 8.

CONCLUSION

In this study, ATG was synthesized from TG and utilized as a carrier in the solid dispersion formulation of KTZ. Compared to the pure medication and TG, the solid dispersion with ATG had enhanced solubility and dissolution. Overall, our work shows that ATG has a promising future as a carrier for the creation of KTZ-loaded SD and fast-dissolving tablets. The findings contribute to the development of efficient drug delivery systems by offering useful insights into methods for improving the solubility and bioavailability of medications that are poorly soluble.

REFERENCES

1. Peyton LR, Gallagher S, Hashemzadeh M. Triazole antifungals: a review. Drugs Today. 2015 Dec 1;51(12):705-18.
2. Hiendrawan S, Hartanti AW, Veriansyah B, Widjojokusumo ED, Tjandrawinata RR. Solubility enhancement of ketoconazole via salt and cocrystal formation. Int J Pharm Pharm Sci. 2015 Jul 1;7(7):160-4.
3. Rodge PJ, Shirolkar SV. Solubility Enhancement of Itraconazole by Centrifugal Melt Spinning Technique. International Journal of Drug Delivery Technology. 2023;13(3):812-817.
4. Pawar SR, Barhate SD. Solubility enhancement (Solid Dispersions) novel boon to increase bioavailability. Journal of Drug Delivery and Therapeutics. 2019 Mar 22;9(2):583-90
5. Joseph J, Kanchalochana SN, Rajalakshmi G, Hari V, Durai RD. Tamarind seed polysaccharide: A promising natural excipient for pharmaceuticals. International Journal of Green Pharmacy (IJGP). 2012;6(4).
6. Teixeira-Costa BE, Andrade CT. Natural polymers used in edible food packaging—History, function and application trends as a sustainable alternative to synthetic plastic. Polysaccharides. 2022 Mar;3(1):32-58.
7. Mamatha P, Bhikshapathi DVRN. Preparation and In-vitro Evaluation of Pemigatinib Nanosponges Tablets by Box-Behnken Design. International Journal of Pharmaceutical Quality Assurance. 2023;14(3):791-800.
8. Malviya R, Sundram S, Fuloria S, Subramaniyan V, Sathasivam KV, Azad AK, Sekar M, Kumar DH, Chakravarthi S, Porwal O, Meenakshi DU. Evaluation and Characterization of Tamarind Gum Polysaccharide: The Biopolymer. Polymers. 2021 Sep 7;13(18):3023
9. Yamatoya K, Tabuchi A, Suzuki Y, Yamada H. Tamarind seed polysaccharide: unique profile of properties and applications. Biopolymer-Based Formulations. 2020 Jan 1:445-61.
10. Lang P, Masci G, Dentini M, Crescenzi V, Cooke D, Gidley MJ, Fanutti C, Reid JS. Tamarind seed polysaccharide: preparation, characterisation and solution properties of carboxylated, sulphated and alkylaminated derivatives. Carbohydrate polymers. 1992 Jan 1;17(3):185-98.
11. Kalbhare S, Pawar RK, Redasani VK, Yadav AB, Mohite VR, Kadam VB. Role of Aminated Derivatives of Natural Gum in Release Modulating Matrix System of Losartan Potassium. International Journal of Pharmaceutical Sciences and Nanotechnology (IJPSN). 2022 Dec 12;15(6):6204-15.
12. Shukla AK, Bishnoi RS, Kumar M, Fenin V, Jain CP. Applications of tamarind seeds polysaccharide-based copolymers in controlled drug delivery: An overview. Asian J. Pharm. Pharmacol. 2018;4:23-30.
13. Kumar CS, Bhattacharya S. Tamarind seed: properties, processing and utilization. Critical reviews in food science and nutrition. 2008 Jan 2;48(1):1-20.
14. Nayak AK, Pal D. Functionalization of tamarind gum for drug delivery. Functional biopolymers. 2018:25-56.
15. Mali KK, Dhawale SC, Dias RJ, Ghorpade VS. Delivery of drugs using tamarind gum and modified tamarind gum: A review. Bulletin of Faculty of Pharmacy, Cairo University. 2019 Jun 1;57(1):1-24.
16. Mahavarkar RV, Ahirrao S, Kshirsagar S, Rayate V. Formulation and evaluation of tamarind seed polysaccharide matrix tablet. Pharm Biol Eva. 2016 Apr 22;3:241-55.
17. Nagaraja K, Krishna Rao KS, Zo S, Soo Han S, Rao KM. Synthesis of novel tamarind gum-co-poly (acrylamidoglycolic acid)-based pH responsive semi-IPN hydrogels and their Ag nanocomposites for controlled release of chemotherapeutics and inactivation of multi-drug-resistant bacteria. Gels. 2021 Nov 27;7(4):237.
18. Butreddy A, Sarabu S, Almutairi M, Ajjarapu S, Kolimi P, Bandari S, Repka MA. Hot-melt extruded hydroxypropyl methylcellulose acetate succinate based amorphous solid dispersions: Impact of polymeric combinations on supersaturation kinetics and dissolution performance. International Journal of Pharmaceutics. 2022 Mar 5;615:121471.
19. Kulkarni NS, Gite PD, Munde MK, Dhole SN, Khiste RH. A comprehensive review on application of microwave irradiation for preparation of inclusion complexes with cyclodextrins. Research

Journal of Pharmacy and Technology. 2021;14(2):1131-6.
20. Bukkawar A, Jain AK, Chatap VK. Formulation Development and Evaluation of Freeze-dried Aviptadil injection using Mannitol as Cryoprotectant. International Journal of Pharmaceutical Quality Assurance. 2023;14(3):541-547.
21. Kolimi P, Youssef AA, Narala S, Nyavanandi D, Dudhipala N, Bandari S, Repka MA. Development and characterization of itraconazole non-aqueous creams for the treatment of topical fungal infections. Journal of Drug Delivery Science and Technology. 2022 Oct 1;76:103818.